

**THE EFFECTS OF POLYMER-CONTROLLED HYDRATION ON
NUCLEAR MAGNETIC RESONANCE PARAMETERS.**

Irene M. Lees

B. Sc. (Physics), University of New Brunswick, 1991

A THESIS SUBMITTED IN PARTIAL FULFILLMENT OF
THE REQUIREMENTS FOR THE DEGREE OF
MASTER OF SCIENCE

in

THE FACULTY OF GRADUATE STUDIES

DEPARTMENT OF PHYSICS

We accept this thesis as conforming
to the required standard

THE UNIVERSITY OF BRITISH COLUMBIA

April 1993

© Irene M. Lees

Abstract

The polymer polyethylene glycol (PEG) was used to control the amount of hydration in lipid bilayers. These bilayers were composed of either 1,2-dimyristoyl-*sn*-glycero-3-phosphocholine (DMPC) or 1,2-dipalmitoyl-*sn*-glycero-3-phosphocholine (DPPC) and oriented between glass slides. These lipids were deuterated in the headgroup to allow their study with ^2H Nuclear Magnetic Resonance (NMR). Specifically, the quadrupolar splitting ($\Delta\nu_q$), the gel to liquid crystalline phase transition temperature (T_m), the spin-lattice relaxation times and the spin-spin relaxation times were investigated as the membrane was dehydrated. Both $\Delta\nu_q$ and T_m are hydration dependent but no systematic change in the relaxation times was noted as a function of the water content of the sample. The spin-spin relaxation times did show an orientation dependence. The analysis led to the proposal that thickness fluctuations and thermal undulations of the membrane were two possible mechanisms for this relaxation.

Table of Contents

Abstract	ii
List of Tables	v
List of Figures	vi
Acknowledgements	vii
1 Introduction	1
2 Lipid Bilayers	3
2.1 Properties of Lipid Bilayers	3
2.2 Motions within Lipid Bilayers	4
2.3 Hydration	5
3 Theory	8
3.1 Spectra of Bilayers	8
3.2 Relaxation	9
3.3 Orientation Dependence of Relaxation	9
4 Experimental Procedure	11
4.1 Equipment	11
4.2 Data Acquisition	11
4.2.1 Quadrupolar Echo	11
4.2.2 Inversion Recovery	13

4.2.3	T_{2qe} Measurements	13
4.2.4	Jeener-Broekaert	14
4.3	Sample Preparation	15
4.4	Depaking	16
5	Results	17
5.1	Quadrupolar Splitting	17
5.2	Transition Temperature	20
5.3	Longitudinal Relaxation Times	23
5.4	Transverse Relaxation Time	26
5.5	Errors	31
6	Discussion	32
7	Conclusion	36
	Bibliography	37

List of Tables

3.1	Legendre Coefficients for Slow Motions	10
4.1	Example τ_1 values	15
4.2	τ_1 Values Used in Experiments	15
5.1	Quadrupolar Splittings for DMPC	19
5.2	Transition Temperature for DMPC	20
5.3	Average T_{1z}	26
5.4	T_2 Fits to Legendre Polynomials	28
5.5	T_2 Fits to $(P_2(\cos \theta))^2$ and $\sin^2 \theta \cos^2 \theta$	29
6.1	Conversion of wt. % PEG to H ₂ O molecules	33

List of Figures

2.1	Structure of DPPC	4
4.1	Stack Plot of Temperature	12
5.1	Quadrupolar Splitting for DPPC	18
5.2	Transition Temperature for DPPC	21
5.3	Relation Between T_m wt. % PEG	22
5.4	Zeeman Spin-Lattice Relaxation Times for DPPC	23
5.5	Zeeman and Quadrupolar Spin-Lattice Relaxation Times for DMPC	25
5.6	Longitudinal Relaxation Times for DMPC	27
5.7	T_2 Fits	30

Acknowledgements

I would like to thank my supervisor, Dr. Myer Bloom, for all his help and support on this project. I felt that I have learned a lot over the past two years.

I would also like to thank Clare Morrison for all her help since many of the ideas came from the work that she was doing. I would also like to express my gratitude to her since she took time out of her busy schedule to show me how things worked in the lab.

The Room 100 bunch was a great pleasure to work with since everyone is so open and friendly. It made the more tedious portions of the two years much more endurable and the exciting parts much more fun. Good luck to all of you in the future.

I would also like to thank the people who helped me out by proof reading my thesis, namely Jeff and Jeff. I hope there aren't too many mistakes left in it.

Finally, I would like to thank my parents who started me out at a young age on the road to science and gave me support from the beginning.

Chapter 1

Introduction

In the past, there have been numerous experiments looking into the effects of hydration on phospholipid bilayers. These experiments include the study of changes in spin-lattice relaxation rates [Ulri 90], measurement of the quadrupolar splittings of the deuterium nuclei [Bech 91] and the determination of the gel to liquid crystalline transition temperature [Jurg 83], all as a function of the water content of the sample. Other experiments have shown that polymers can be used to change the hydration of a bilayer [LeNe 77]. Polyethylene glycol (PEG) is a polymer which is known to form many hydrogen bonds and therefore water binds to the polymer surface. In fact, at 38 wt. % PEG and above, no free water exists in the mixture. This fact makes PEG ideal as a dehydrating agent in membrane experiments since it is easy to control and may simply be added to the sample. This polymer has been used as a dehydrating agent in other experiments such as protein crystallization and membrane fusion [MacD 85] but so far it has not been used in conjunction with NMR relaxation studies of membranes. Furthermore, several studies have shown that PEG, with a sufficiently high molecular weight, is excluded from the surface of bilayers and therefore does not physically enter the membrane thereby causing bilayer disruption [Arno 90]. This fact is also supported by consistent NMR results between samples with and without PEG added.

The initial findings support the theory that PEG can be used to dehydrate membranes since the NMR results using PEG are similar to results using other methods of membrane dehydration. Since the addition of a polymer to a lipid sample is relatively simple, this

method of dehydrating should prove useful in the future in studying the effects of low water content on the properties of lipid bilayers.

Chapter 2

Lipid Bilayers

2.1 Properties of Lipid Bilayers

The main function of a membrane is to compartmentalize different areas of cells and to serve as a semi-permeable barrier. Cell membranes are composed of lipids and proteins, where the lipids provide the structure and the proteins carry out the functions of the membrane such as ion transport, energy production, etc. In this study, only model membranes were used since real cell membranes are much more complicated and results are difficult to interpret.

A model membrane composed of only one type of lipid was used. Lipids are amphiphilic in nature (i.e. they have both a hydrophobic and a hydrophilic domain). Therefore, when placed in water, they tend to form bilayers with the hydrophilic polar headgroup facing out towards the water and the hydrophobic tails facing the inside of the bilayer. The strain on the ends of the bilayer due to the hydrophobic core coming into contact with the surrounding water causes the bilayers to fold into spherical vesicles.

The two types of lipids used in this study were 1,2-dimyristoyl-*sn*-glycero-3-phosphocholine (DMPC) and 1,2-dipalmitoyl-*sn*-glycero-3-phosphocholine (DPPC). These lipids were deuterated in the α , β and γ positions of the headgroup defined in Figure 2.1. DMPC has a very similar structure except that the chains are 14 carbons long instead of 16 carbons.

One fundamental property of lipids is a phase transition from a gel phase at low

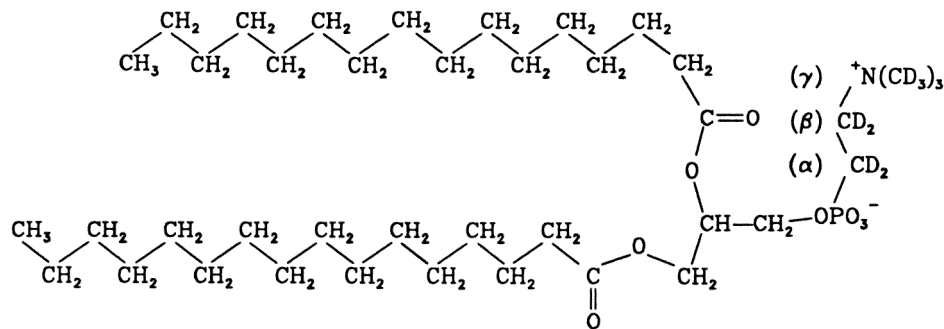


Figure 2.1: **Structure of DPPC**

The structure of DPPC is shown as well as the thirteen deuterons associated to the α , β and γ positions.

temperature, involving slow lateral diffusion of the lipids and excitation of very few trans-gauche isomerizations in the hydrocarbon chains, to the liquid crystalline phase at high temperature, where faster lateral diffusion is allowed and many kinks are formed along the hydrocarbon chains. This phase transition can be monitored using NMR since each phase has a distinct spectral signature.

2.2 Motions within Lipid Bilayers

There are many different types of motions in bilayers which occur over a wide range of timescales. Such motions include lateral diffusion (i.e. lipids moving in the plane of the bilayer), rotational diffusion about the long axis of the lipid molecule, lipid flip-flop from one side of the bilayer to the other, trans-gauche isomerization in the hydrocarbon chains, headgroup motions, movement of the lipids into or out of the plane of the bilayer and thermal undulations [Pfei 89]. Many of these motions contribute to the relaxation rates in NMR and therefore measurement of different relaxation times can be used to determine the time scales of the lipid motion.

One type of motion which is important in NMR spectra of powder samples is lateral

diffusion of the lipids around the vesicle. This diffusion causes complications in the interpretation of the spin-spin relaxation times (T_2) since a variety of angles are sampled by the lipid during the length of the experiment. Since T_2 times are orientation dependent, the true T_2 relaxation rate can not be determined. In order to remove the effects of diffusion, bilayers are oriented between glass plates so that movement of the lipids will only be along one plane. The lateral diffusion will now no longer affect the spectrum since the angle between the bilayer normal and the main magnetic field will not change as the lipids diffuse. This allows the study of other types of motions in the membrane.

2.3 Hydration

In recent years, several groups have looked into the interactions of water with bilayers. There appear to be three water layers associated with a fully hydrated bilayer [Fine 74]. The first is a layer of water very strongly bound to the headgroups. There is also an intermediate water phase where water is present between the stacked bilayers. This second layer is quite free to move but it is rapidly exchanged with the bound water. Finally, there is a bulk water phase where water has unrestricted movement and is not directly associated with the bilayer. The actual number of water molecules associated with each of these three phases varies from lipid to lipid depending on the size and charge of the headgroup.

A previous study [Bush 80] showed that for DPPC, the first two water molecules added to the lipid separate and shield the phosphate charges from one another. Also, their results indicate that these water molecules are not strongly hydrogen bonded to the phosphate oxygen atoms but instead the PO_4^- group is free to rotate. The conformation of the headgroup seemed to be determined from the first four or five water molecules added to the lipid since, after this, no further headgroup reorientation occurs. This is

not consistent with other findings [Bech 91] which indicate that a change in the headgroup orientation does occur at higher levels of hydration.

In vivo biological membranes are found in a state of full hydration, defined as the state where no change in any of the physical properties of the membrane occurs with the addition of water. Therefore, experiments which attempt to mimic *in vivo* situations should also use fully hydrated membranes. Actual methods of obtaining a fully hydrated membrane seem to be under dispute.

When using oriented samples, it is not possible to add a large amount of bulk water to the sample since the lipids detach from the glass slides and form vesicles thereby ruining the orientation of the sample. Therefore, there is some problem in achieving full hydration in these bilayers. The most common way of getting a hydrated membrane is to leave the lipids in a water saturated vapour for a varying length of time (from hours to days) so that the bilayer absorbs water. Recent studies [Rand 89] have shown that this method does not lead to full hydration. In fact, only a 35 wt. % hydration is achieved whereas full hydration is estimated at greater than 50 wt. % hydration. Thus, a new method needs to be developed in order to ensure full hydration in oriented bilayers.

In this study, a polymer (PEG) was used to hydrate the membrane. PEG has the chemical structure



and water is found hydrogen bonded to the oxygen. Since both the membrane and the polymer competed for the water in the sample, the addition of bulk water without the lipids forming vesicles and sample orientation being lost was allowed. With only a small amount of PEG added to the sample, the membrane was very close to full hydration. Larger amounts of polymer can also be added to dehydrate the membrane so that studies on water depleted bilayers can be carried out.

Although PEG was not used as a dehydrating agent, studies on dehydrated powder bilayers have been done in the past [Bech 91,Ulri 90,Jurg 83]. Therefore, this study was compared to previous results to determine whether PEG produced the same effects when used for bilayer dehydration.

One effect of bilayer dehydration is a change in the transition temperature from the gel to the liquid crystalline phase. The phase diagram for DPPC at low water concentrations has been determined [Jurg 83]. Another group [Cevc 85] theorized that, at low water concentrations, the shift in transition temperature from that of a fully hydrated bilayer was directly proportional to the number of water molecules associated with each lipid.

Bechinger and Seelig [Bech 91] recently determined the effects of dehydration on the quadrupolar splitting of deuterons in the headgroup of 1-palmitoyl-2-oleoyl-*sn*-glycero-3-phosphocholine (POPC). The changes in $\Delta\nu$ are attributed to conformational changes in the headgroup due to lower amounts of water in the surrounding environment.

Another study evaluated the effect of hydration on spin-lattice relaxation times (T_1) [Ulri 90]. The results showed an almost linear increase in the T_1 relaxation times as water was added until full hydration was achieved at approximately 22 water molecules per lipid after which the relaxation times levelled off to their value at full hydration.

Chapter 3

Theory

3.1 Spectra of Bilayers

In nuclei with spin greater than one, there is an interaction between the quadrupole moment and the local electric field gradient at the nucleus. This is the dominant effect on the ^2H NMR spectra.

The ^2H NMR spectrum of an immobilized C- ^2H bond making an angle Θ with respect to the main magnetic field is a doublet with splitting $2\omega(\Theta)$ where

$$\omega(\Theta) = \omega_q P_2(\cos \Theta) = \omega_q (3 \cos^2 \Theta - 1)/2 \quad (3.1)$$

In the case of deuterium, $\frac{\omega_q}{2\pi} \simeq 125\text{kHz}$. (Note that the influence of a small deviation from axial symmetry was neglected in writing Eq. 3.1 [Davi 83].)

In the presence of axially symmetric motions fast on the NMR timescale, the quadrupolar splittings only depend on θ (the angle between the magnetic field and the surface normal of the bilayer). Therefore,

$$\omega(\theta) = \langle \omega(\Theta) \rangle_{\text{fastmotions}} = \omega_q S_{CD} (3 \cos^2 \theta - 1)/2 \quad (3.2)$$

where S_{CD} is known as the order parameter and is equal to

$$S_{CD} = \langle (3 \cos^2 \beta - 1)/2 \rangle_{\text{fastmotions}} \quad (3.3)$$

Here, β is defined as the angle between the surface normal of the bilayer and the C- ^2H bond.

3.2 Relaxation

There are two different types of relaxation that occur in NMR. The *first* is known as spin-lattice or longitudinal relaxation and it is characterized by a relaxation time T_1 . This relaxation is due to spin flips which cause one or two quanta of Zeeman energy to be exchanged between the spin and the lattice. These processes involve spectral densities associated with frequencies near the Larmor frequency $\omega = \omega_0$ and twice the Larmor frequency $\omega = 2\omega_0$, respectively. The *second* is known as spin-spin relaxation and it is characterized by a relaxation time T_2 . This relaxation is due to the loss of phase memory by the spins due to thermally driven fluctuations in the quadrupolar splittings. T_1 is affected by fast motions on the NMR timescale whereas T_2 is affected by both fast and slow motions. It can be shown that $T_2 \leq T_1$.

3.3 Orientation Dependence of Relaxation

A general expression for the orientation dependence of T_i (T_{1z} , T_{1q} or T_2) for fast motions has been derived by Morrison and Bloom [Morr 93a]. It takes the form,

$$\frac{1}{T_i} = \sum_{p=0}^4 \sum_{q=-p}^p a_{pq}^{(i)} Y_{pq}(\theta, \phi) \quad , p \text{ even} \quad (3.4)$$

For the case of axial symmetry (which is present in liquid crystalline or fluid lipid bilayer systems), this equation can be reduced to a sum of even Legendre polynomials up to order 4, i.e.

$$\frac{1}{T_i} = a_0 + a_2 P_2(\cos \theta) + a_4 P_4(\cos \theta) \quad (3.5)$$

The coefficients are functions of order parameters and correlation times and indicate the types of motion present in the system.

For special mechanisms of slow motion, specific orientation dependencies of the relaxation rates can be derived. Two such mechanisms are surface undulations whose angular

Table 3.1: Legendre Polynomial Coefficients for Example Motions

Motion	Parameter	Value
$(P_2(\cos \theta))^2$	a_0	0.20
	a_2	0.29
	a_4	0.51
$\sin^2 \theta \cos^2 \theta$	a_0	0.13
	a_2	0.095
	a_4	-0.23

dependence is predicted to be proportional to $\sin^2 \theta \cos^2 \theta$ [Blo 91a] and thickness fluctuations proportional to $(P_2(\cos \theta))^2$ providing that they occur without any change in membrane orientation [Bloom, private communication]. These two expressions can be rewritten to be expressed as a sum of Legendre polynomials with specific coefficients (see Table 3.1).

Chapter 4

Experimental Procedure

4.1 Equipment

The equipment used to obtain all experimental data was a home-built spectrometer [Ster 85] at 46 MHz. The 90° pulse length was equal to $4 \mu\text{s}$ and the dwell time was set to $5 \mu\text{s}$. The signal was acquired in quadrature with cyclops phase cycling to increase the signal to noise ratio [Davi 79].

The temperature was regulated with a Bruker Model BV T1000 temperature controller and was measured to an accuracy of ± 0.5 degrees.

The sample orientation was controlled using a home-built goniometer accurate to ± 0.5 degrees.

4.2 Data Acquisition

In order to determine the parameters under study, a variety of pulse sequences were applied. These enabled the quadrupolar splitting, the transition temperature, the spin-lattice relaxation times and the transverse relaxation time to be measured.

4.2.1 Quadrupolar Echo

The quadrupolar echo pulse sequence used was

$$90_y^\circ - \tau - 90_x^\circ - t$$

where a value of $\tau = 50 \mu\text{s}$ was used for spectroscopic measurements.

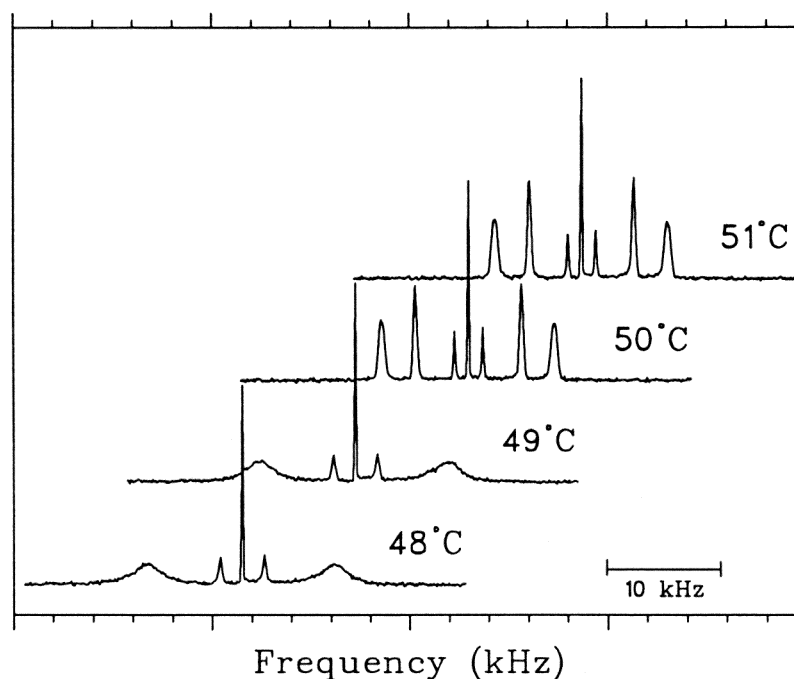


Figure 4.1: **Transition Temperature**

A stacked plot showing the determination of the transition temperature is presented. In this case, T_m was taken as 50°C since at this temperature the peaks became very sharp. This illustrative plot was done for the 60 wt. % PEG sample of DPPC.

The spectra found from this pulse sequence were used to measure the quadrupolar splitting for the three deuteron positions. The spectra were also used to determine the transition temperature for the sample with an accuracy of $\pm 0.5^\circ\text{C}$. The actual value of the transition temperature was taken as the temperature at which the outer peaks in the spectrum became much sharper and narrower (Figure 4.1). The temperature was increased in 1°C steps.

4.2.2 Inversion Recovery

The Zeeman energy spin lattice relaxation time, T_{1z} , was measured using an inversion recovery pulse sequence,

$$180_y^\circ - \tau_1 - 90_y^\circ - \tau_2 - 90_x^\circ - t$$

The signal was actually modified by subtracting the inverted spectrum from the quadrupolar spectrum obtained in the absence of the 180° inverting pulse. This gave a signal which was maximum at $\tau_1 = 0$ and decayed to zero as τ_1 increased. Ten τ_1 values ranging from 1 ms to 90 ms were used. The value of τ_2 remained constant at $50 \mu\text{s}$.

The intensity of the deuteron peaks from the spectra were determined for each τ by Fourier transforming from the peak of the echo. These intensities were fit to an exponential curve

$$M = M_0 e^{-\tau/T_{1z}}$$

where M is the signal intensity and T_{1z} is the longitudinal relaxation time.

4.2.3 T_{2qe} Measurements

The transverse relaxation time, T_{2qe} , was determined using a quadrupolar echo sequence with varying values of τ ,

$$90_y^\circ - \tau - 90_x^\circ - t$$

The values of the nine τ used were between $50 \mu\text{s}$ and 4 ms.

Again, the intensity of the FT spectrum was determined for each τ for each deuteron position. These values were then fit to the exponential

$$M = M_0 e^{-2\tau/T_{2qe}}$$

where M is the signal intensity. The transverse relaxation time, T_{2qe} , could then be determined from the graph.

4.2.4 Jeener-Broekaert

The Jeener-Broekaert pulse sequence [Jeen 67] was used to measure the quadrupolar relaxation time for the DMPC sample. This pulse sequence consists of

$$90_x^\circ - \tau_1 - 45_y^\circ - \tau_2 - 45_y^\circ - t$$

Different values of τ_1 cause a modulation proportional to $\sin(\omega_q \tau_1)$ in the amplitude of the signal [Bloo 91b], where ω_q is equal to $2\pi\Delta\nu_q$. Therefore, if

$$\omega_q \tau_1 = \frac{\pi}{2}$$

then the signal will be a maximum. This is equivalent to choosing τ_1 values according to

$$\tau_1 = \frac{1}{4\Delta\nu_q}$$

where $\Delta\nu_q$ is the quadrupolar splitting frequency of the deuterons. In order to avoid running three experiments for the three types of deuterons each with different $\Delta\nu_q$, the τ_1 value had to be optimized for all three deuterons at once. To do this, the τ_1 value was calculated for each deuteron at a specific angle. The experimental τ_1 value was then chosen close to the optimum values for α and β since the γ deuterons had a much larger signal and could afford the reduced intensity. An example of a choice of τ_1 is shown in Table 4.1 where τ_1 was chosen as 50 μs since it is intermediate to all three individual values although biased towards α and β . The actual τ_1 value for each bilayer orientation used is shown in Table 4.2. The τ_2 times ranged from 1 ms to 150 ms.

The spectra were obtained by Fourier transforming the FID signal from the first zero crossing. The T_{1q} relaxation times were found for each deuteron position by fitting the FT intensities to an exponential (i.e. the same procedure used in the determination of T_{1z}).

Table 4.1: **Example of a chosen τ_1 value for 0° orientation.**

Deuteron	$\Delta\nu$	calculated τ_1	chosen τ_1
α	6.379	39 μs	50 μs
β	5.383	46 μs	
γ	1.256	199 μs	

Table 4.2: **Jeener Broekaert pulse sequence τ_1 values**

Angle θ	τ_1 (μs)
0°	50
15°	50
30°	60
45°	130
75°	130
90°	80

4.3 Sample Preparation

DPPC-d₁₃ and DMPC-d₁₃, specifically deuterated in the α , β and γ positions of the headgroup, were purchased from Avanti Polar Lipids Inc. (Birmingham, Al.). The two different molecular weights of PEG (3000 and 8000) were purchased from Sigma Chemical Company (St. Louis, MO, U.S.A.).

The powder sample was made by dissolving 50 mg of DMPC in 1 mL of chloroform. Most of the chloroform was then evaporated to produce a thin film of lipid at the bottom of the test tube. The sample was then placed in a lyophilizer overnight to pump off the rest of the chloroform. The sample was freeze-thawed by cooling in liquid nitrogen for half an hour, then heating above T_m and vortexing. This was done three times and then approximately 500 μL of deuterium depleted water was added. The solution was then transferred to an NMR tube (10 mm o.d.) and placed in the spectrometer for study.

Oriented samples were prepared by dissolving 10 mg of lipid for the DPPC or 20 mg for the DMPC in 100 μL or 200 μL of chloroform, respectively. The lipid was then spread on approximately 20 glass slides (of dimensions 5 mm x 1.5 mm) and the chloroform was removed by pumping overnight. The samples were then hydrated at 50°C in a water saturated vapour environment for 48 hours. The slides were stacked and wrapped with teflon tape to squeeze the slides together. Next, the samples were placed inside an NMR tube (10 mm o.d.) and were again placed in the water saturated vapour for another 24 hours. Approximately 500 μL of PEG-water solution was added to immerse the slides and the sample was left for 24 hours to allow the water to reach equilibrium between the PEG and the lipids. The samples were sealed and placed in the NMR probe where the experiments were carried out.

The PEG solutions were made by adding PEG to deuterium depleted water at concentrations varying between 5 wt. % and 80 wt. %. These solutions were heated slightly to ensure that the PEG was fully and uniformly dissolved. The definition of weight % was taken as the mass of the PEG over the total mass of the solution (i.e. the mass of the PEG plus the mass of the water) times 100%.

4.4 Depaking

DePaking was performed using the DePaking procedure [Ster 83] on the spectra acquired from the powder sample in order to resolve the individual peaks of the three deuteron positions.

Chapter 5

Results

5.1 Quadrupolar Splitting

The quadrupolar splitting ($\Delta\nu_q$) for each of the α , β and γ deuterons was determined for the DPPC samples at a variety of PEG concentrations (Figure 5.1). All the DPPC experiments were carried out at the 0° orientation. The results show that $\Delta\nu_q$ for the α position increases as the bilayer hydration decreases. The opposite is true for the β deuterons where $\Delta\nu_q$ increases as the amount of water in the bilayer decreases. For the γ deuterons, $\Delta\nu_q$ remains constant as water is removed from the lipids. When comparing the results for the 3000 and 8000 molecular weight PEG, there appears to be very little difference between the quadrupolar splittings. This would tend to indicate that both polymers are dehydrating the membrane by the same amount.

When examining the DMPC samples, the splitting associated with the dePaked powder spectrum peaks (which is equivalent to the 0° orientation) was also determined and used as a comparison between a fully hydrated system and a system with different levels of dehydration (Table 5.1). These quadrupolar splittings are equivalent to

$$\Delta\nu_q = \nu_q S_{CD} \frac{3 \cos^2 \theta - 1}{2} \quad (5.1)$$

where S_{CD} was defined in chapter 3 as the order parameter and ν_q is 125 kHz for C-D bonds [Davi 83]. For low PEG concentrations, the quadrupolar splittings between the powder samples and the PEG-treated samples at 0° were approximately the same, indicating that full hydration was present as far as $\Delta\nu_q$ can measure.

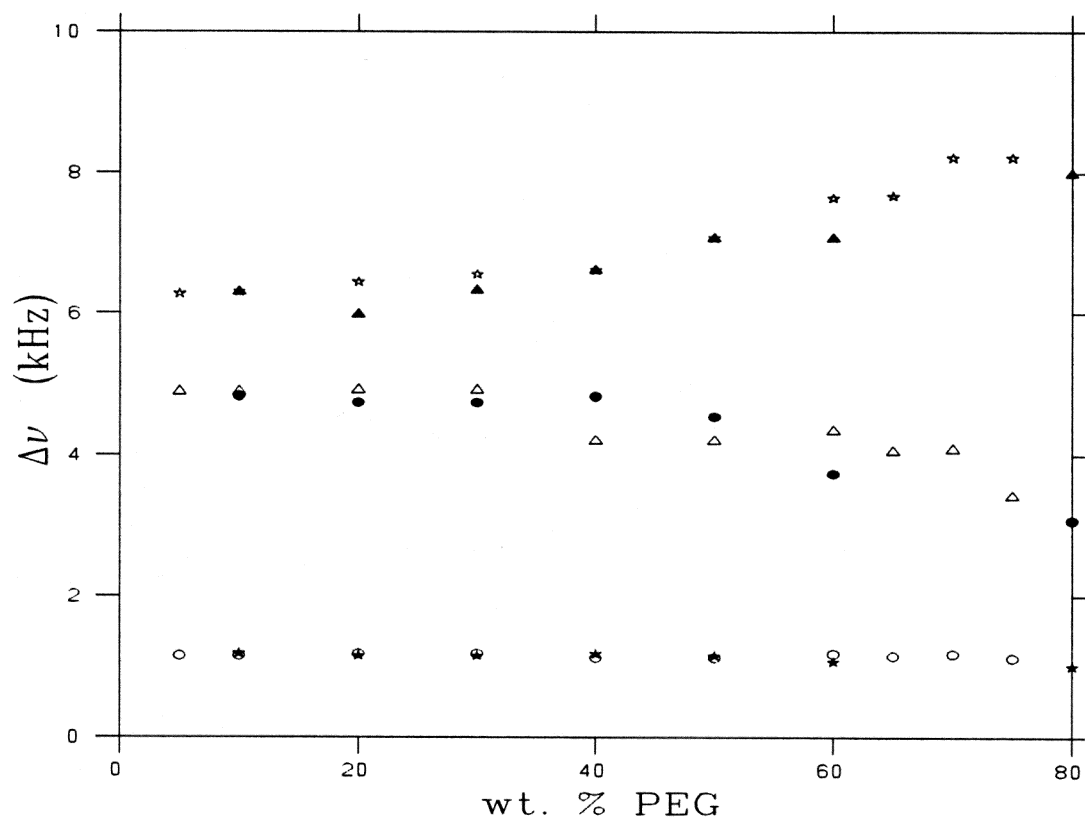


Figure 5.1: **Quadrupolar Splitting for DPPC**

The quadrupolar splitting are shown for the deuterons of DPPC for both the 3000 and 8000 molecular weight PEG. The open symbols refer to the 8000 mw PEG and the solid symbols to the 3000 mw PEG. From top to bottom, the $\Delta\nu_q$ correspond to the α , β and γ deuterons. The samples were all placed at the 0° orientation.

Table 5.1: Quadrupolar splittings for DMPC

Orientation	Deuteron	$\Delta\nu_q$ (kHz)	
		5 wt. %	50 wt. %
dePaked powder (0°)	α	6.336	
	β	5.344	
	γ	1.298	
0°	α	6.379	7.505
	β	5.383	4.705
	γ	1.256	1.227
15°	α	5.975	6.898
	β	5.008	4.474
	γ	1.184	1.126
30°	α	4.315	5.124
	β	3.622	3.320
	γ	0.847	0.852
45°	α	2.511	2.425
	β	2.078	1.559
	γ	0.505	0.404
75°	α	2.006	2.194
	β	1.689	1.414
	γ	0.419	0.376
90°	α	3.132	3.579
	β	2.612	2.353
	γ	0.621	0.621

Table 5.2: Transition Temperatures for DMPC

sample	T_m ($^{\circ}\text{C}$)
powder	24
5 wt. %	24
10 wt. %	24
50 wt. %	28

5.2 Transition Temperature

The transition temperature, T_m , from the gel phase to the liquid crystalline phase for the bilayer is hydration dependent (Figure 5.2). As the amount of water associated with the lipid bilayer decreases, the transition temperature rises. The transition temperature is unaffected by only slight dehydration since T_m remains constant for samples with up to 30 wt. % PEG. At higher PEG concentrations, the transition temperature does rise as the level of dehydration increases in the membrane. There appears to be little difference in the effects of 3000 and 8000 molecular weight on transition temperature which again indicates that both polymers seem to affect the membrane in the same manner. There appears to be a direct relationship between the transition temperature and the square of the PEG concentration (Figure 5.3).

For the DMPC samples, the transition temperature was determined first so that each sample could be maintained at a consistent number of degrees above T_m during the subsequent experiments. Therefore, the $\Delta\nu_q$, the T_{1z} relaxation and the T_{2qe} relaxation experiments were all done at sixteen degrees above the phase transition temperature. The transition temperature values for DMPC are shown in Table 5.2.

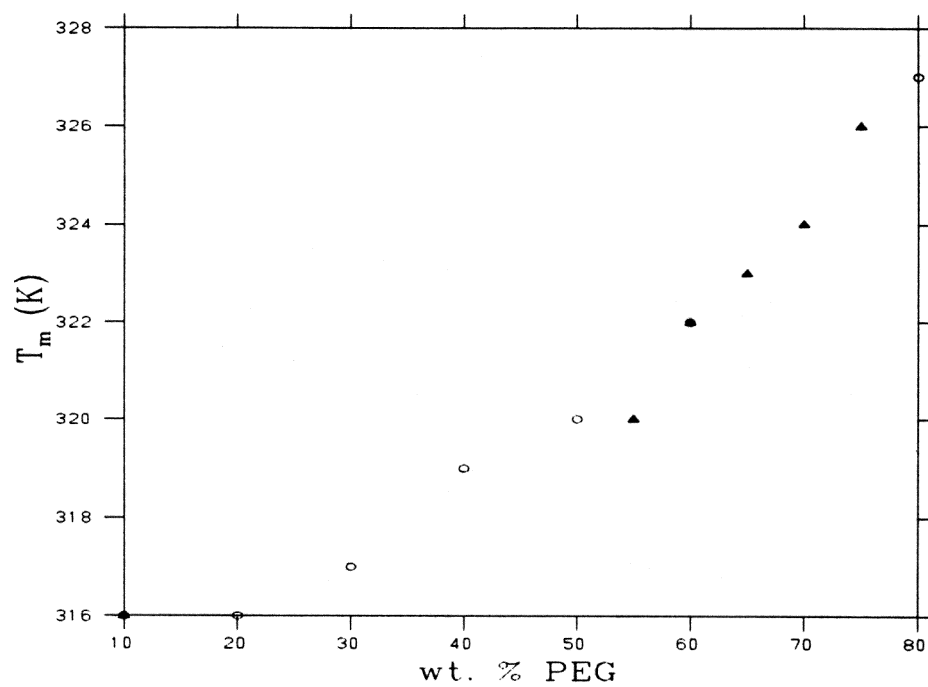


Figure 5.2: **Transition Temperature for DPPC**

The gel to liquid crystalline transition temperature in DPPC for 3000 and 8000 molecular weight PEG is plotted as a function of wt. % PEG. The open symbols refer to the 3000 mw PEG and the solid symbols to the 8000 mw PEG.

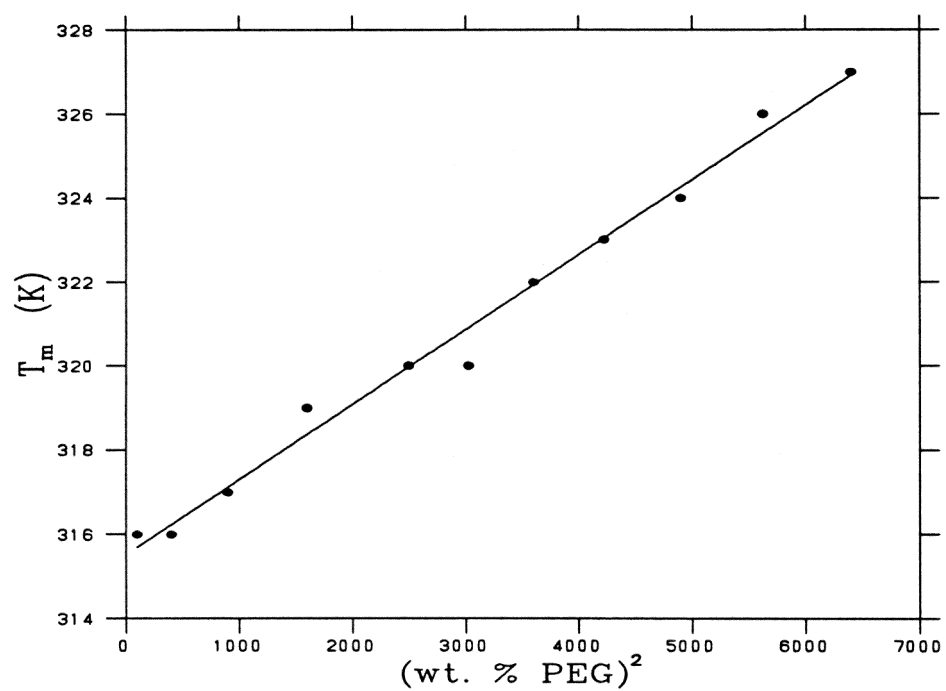


Figure 5.3: **Transition Temperature vs $(\text{wt. \% PEG})^2$ for DPPC**
The transition temperature for DPPC is plotted as a function of $(\text{wt. \% PEG})^2$. A linear fit is made with a slope of 0.00178.

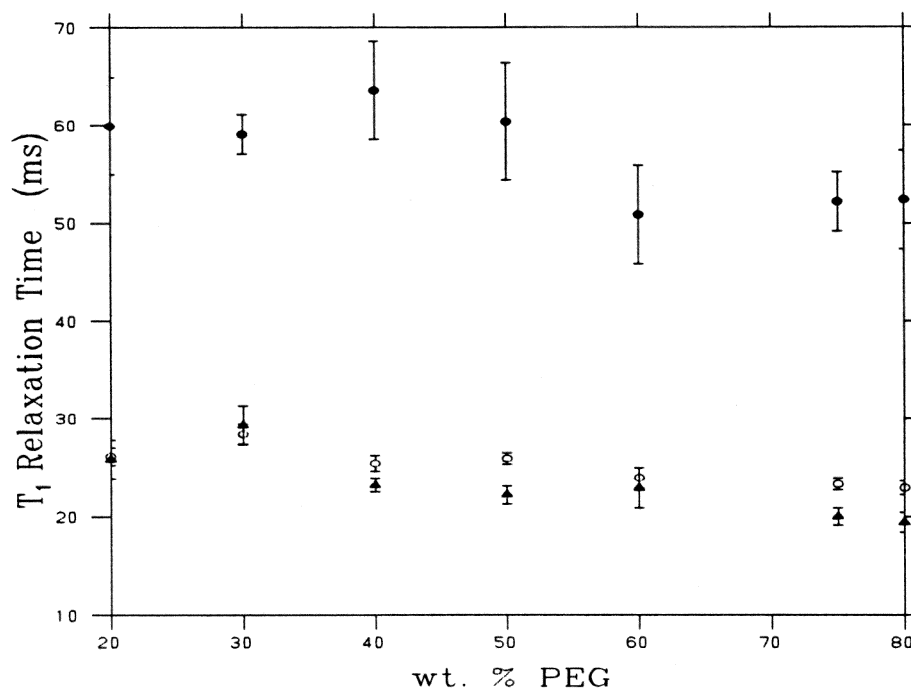


Figure 5.4: **Spin-lattice Relaxation Times for DPPC**

The Zeeman spin-lattice relaxation times for DPPC are determined as a function of the wt. % PEG. The triangles correspond to the α deuterons, the open circles to the β deuterons and the solid circles to the γ deuterons. The samples were at 0° orientation.

5.3 Longitudinal Relaxation Times

The T_{1z} relaxation times were studied for both DPPC and DMPC and the T_{1q} relaxation times were found for DMPC. T_{1q} was measured as well as T_{1z} , for the DMPC case, in order to obtain a larger number of parameters which would lead to a more accurate determination of the motions present in the sample. These relaxation times were obtained as detailed in chapter 4.

The results for the DPPC samples are shown in Figure 5.4. These results were again taken at 0° orientation only. There was a small decrease in the T_{1z} relaxation time as the sample was dehydrated (approximately 20%).

For DMPC, the orientation dependence of the T_{1z} and T_{1q} relaxation times, reflecting the anisotropy, was determined for each deuterium position. The values indicate that there is not much anisotropy since relaxation times vary only slightly with orientation (Figure 5.5). At 5 wt. % PEG, the T_{1z} relaxation times for the α and β deuterons were quite similar with values around 25 ms but the γ deuteron had a longer relaxation time at about 65 ms. The T_{1q} relaxation times were longer than the T_{1z} values but the same general orientation dependence was observed. In this case, the T_{1q} relaxation times for the α and β deuterons were both about 38 ms, while T_{1q} was 105 ms for the γ deuteron. For the 30 wt. % sample, the relaxation times were slightly lower for both T_{1z} and T_{1q} (by about 10%) but again only a slight anisotropy was noticed in the orientation dependence. It should be noted that theory predicts that

$$\frac{T_{1z}}{T_{1q}} = \frac{5}{3}, \quad \omega_0\tau_c \ll 1 \quad (5.2)$$

which is consistent with the results here taking into account experimental error.

The relaxation times of the powder sample were compared to the relaxation times of the PEG samples to see whether full hydration was achieved using a sample containing PEG. In order to compare these values, the T_{1z} values for the oriented samples were averaged over orientation. A straight averaging was not done since the angles chosen for study were not at exact intervals of $\cos\theta$. Instead, a $\sin\theta$ weighted average was taken by fitting a straight line to the T_{1z} vs $\sin\theta$ curve and then averaging points at equal intervals along this line. The results are shown in Table 5.3. Since the relaxation times at low PEG concentration are similar to the ones from the powder sample, full hydration is probably achieved for the 5 wt. % PEG sample insofar as can be ascertained by spin-lattice relaxation.

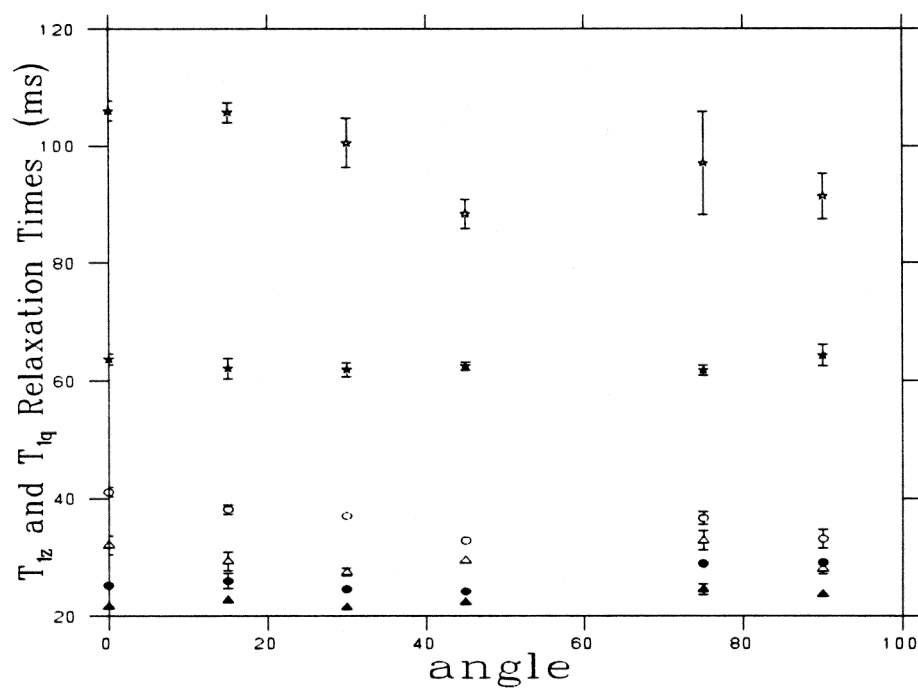


Figure 5.5: **Spin-lattice Relaxation Times for DMPC**

The Zeeman and quadrupolar spin-lattice relaxation times for DMPC are plotted as a function of orientational angle θ . The solid symbols correspond to the Zeeman relaxation times and the open symbols correspond to the quadrupolar relaxation times. The relaxation times from the bottom to the top correspond to the α , β and γ deuterons, respectively. The sample is at 5 wt. % PEG.

Table 5.3: Average value of T_{1z} Relaxation Times for DMPC

Sample	Position	Average T_{1z} (ms)
powder	α	22.3 ± 1
	β	27.4 ± 4
	γ	63.1 ± 3
5 wt. %	α	23 ± 1
	β	26 ± 2
	γ	63 ± 1
10 wt. %	α	22.6 ± 2
	β	25.1 ± 2
	γ	64.6 ± 0.9
50 wt %	α	21 ± 2
	β	24 ± 2
	γ	60 ± 2

5.4 Transverse Relaxation Time

The orientational dependence of the transverse relaxation time was studied at various degrees of bilayer hydration. The relaxation times were again obtained as described in section 4.2.3.

For the 5 wt. % sample, the relaxation times for each of the α , β and γ deuterons are similar in magnitude although the orientation dependence is slightly different (Figure 5.6). This is also true of the 50 wt. % sample. The values of $1/T_2$ were plotted versus the angle and then fit to a sum of Legendre polynomials up to order four

$$\frac{1}{T_2} = a_0 + a_2 P_2(\cos \theta) + a_4 P_4(\cos \theta). \quad (5.3)$$

This gave three parameters shown in Table 5.4 for each of the deuteron positions. The fits of the experimental data to this equation are reasonable as will be shown later in Figure 5.7D.

In section 3.3, it was seen that specific types of motions could be represented by the

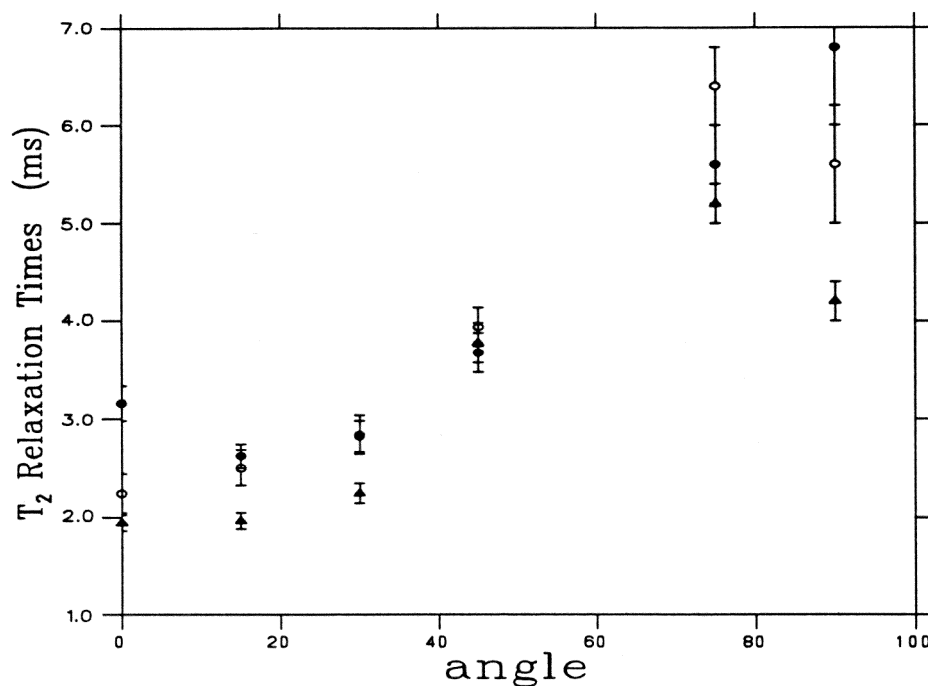


Figure 5.6: **Longitudinal Relaxation Times for DMPC**

The longitudinal relaxation times for DMPC are plotted as a function of orientational angle. The triangles correspond to the α deuterons, the open circles to the β deuterons and the solid circles to the γ deuterons. The sample is at 5 wt. % PEG.

terms $(P_2(\cos \theta))^2$ and $\sin^2 \theta \cos^2 \theta$. From this theory, it was shown that these terms could also be represented by a sum of Legendre polynomials with the coefficients a_0 , a_2 and a_4 shown in Table 3.1. These coefficients indicate that the experimental data can not be fit simply to either $(P_2(\cos \theta))^2$ or $\sin^2 \theta \cos^2 \theta$ since in the case of the experimental data, a_4 is smaller than a_2 while the theoretical values give a_4 larger than a_2 .

Therefore, a linear combination of the two angular dependencies and an isotropic term was fit to the data, i.e.

$$\frac{1}{T_2} = a + b(P_2(\cos \theta))^2 + 4c \sin^2 \theta \cos^2 \theta \quad (5.4)$$

The values for the three parameters are shown in Table 5.5. The choice of $4c$ for the last coefficient was to add a normalization factor since $(P_2(\cos \theta))^2$ has a maximum value

Table 5.4: Fitting of T_2 to a sum of Legendre polynomials

Sample	Position	Parameter	Value
5 wt. %	α	a_0	0.28 ± 0.02
		a_2	0.19 ± 0.03
		a_4	0.07 ± 0.04
	β	a_0	0.24 ± 0.01
		a_2	0.17 ± 0.02
		a_4	0.04 ± 0.02
	γ	a_0	0.24 ± 0.02
		a_2	0.16 ± 0.03
		a_4	-0.04 ± 0.03
50 wt. %	α	a_0	0.15 ± 0.05
		a_2	0.5 ± 0.1
		a_4	0.8 ± 0.4
	β	a_0	0.11 ± 0.03
		a_2	0.33 ± 0.03
		a_4	0.9 ± 0.1
	γ	a_0	0.21 ± 0.03
		a_2	0.03 ± 0.1
		a_4	0.5 ± 0.3

of 1 and $\sin^2 \theta \cos^2 \theta$ has a maximum value of $1/4$. These values could have also been attained by rewriting equation 5.3 in terms of equation 5.4 and determining the a , b and c parameters.

In general, the fit of the previous equation to the data was reasonably close for all the samples except for the γ deuteron at 50 wt. % which showed an entirely different sort of orientation dependence (as can be seen from the unusual coefficients in Table 5.4 and 5.5). The necessity of using a superposition of all motions is demonstrated in Figure 5.7. The best fit is plot D which includes all three parameters.

Table 5.5: **Fitting of T_2 to $(P_2(\cos\theta))^2$ and $\sin^2\theta \cos^2\theta$**

Sample	Position	Parameter	Value
5 wt. %	α	a	0.11 ± 0.05
		b	0.45 ± 0.05
		c	0.15 ± 0.05
	β	a	0.07 ± 0.02
		b	0.38 ± 0.03
		c	0.17 ± 0.03
	γ	a	0.08 ± 0.04
		b	0.27 ± 0.05
		c	0.20 ± 0.04
10 wt. %	α	a	0.15 ± 0.05
		b	0.3 ± 0.1
		c	0.1 ± 0.1
	β	a	0.10 ± 0.05
		b	0.3 ± 0.1
		c	0.2 ± 0.1
	γ	a	0.11 ± 0.04
		b	0.20 ± 0.05
		c	0.15 ± 0.05
50 wt. %	α	a	0.15 ± 0.05
		b	0.5 ± 0.1
		c	0.2 ± 0.1
	β	a	0.11 ± 0.03
		b	0.33 ± 0.03
		c	0.22 ± 0.03
	γ	a	0.21 ± 0.03
		b	0.03 ± 0.1
		c	0.1 ± 0.05

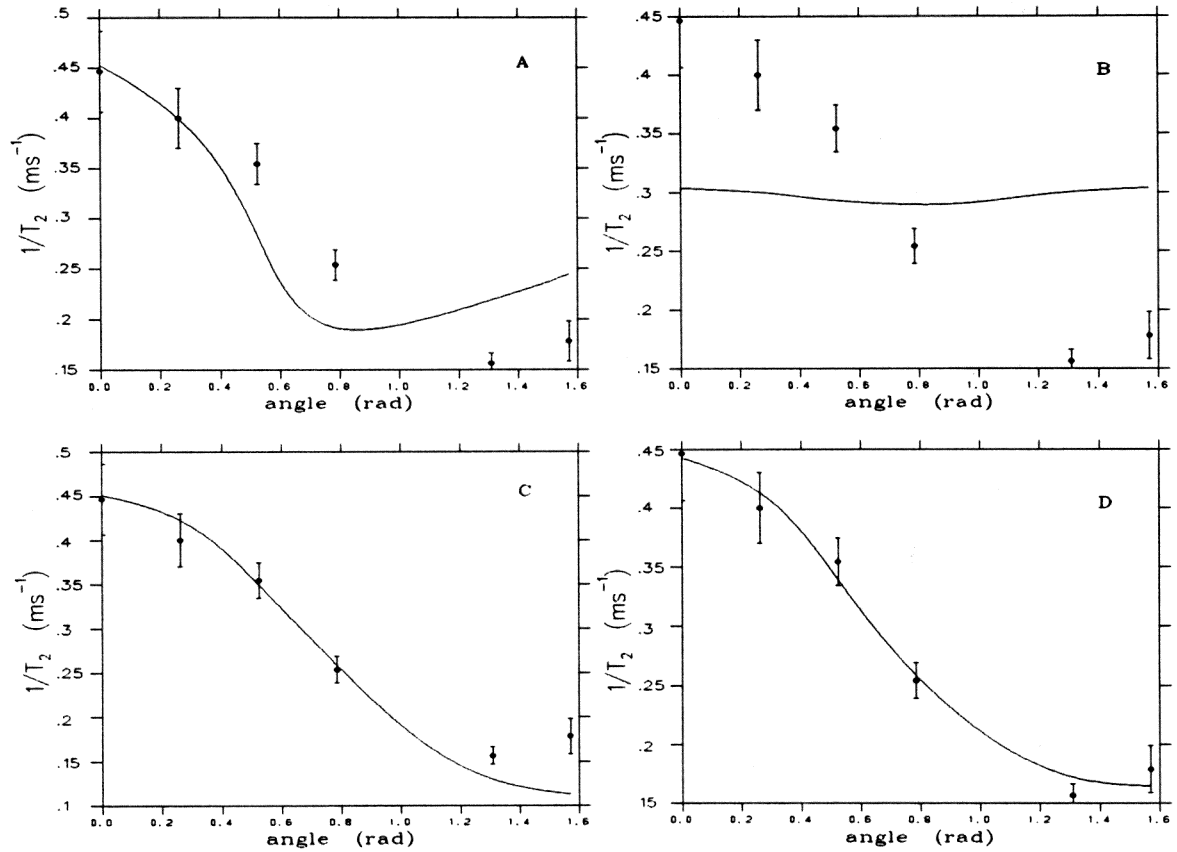


Figure 5.7: **Orientation fits for T_2 Relaxation**

These are fits of $\frac{1}{T_2}$ vs angle for different angular dependencies. The actual fits in the plots are; A: $a + b P_2^2(\cos \theta)$; B: $a + c \sin^2 \theta \cos^2 \theta$; C: $b P_2^2(\cos \theta) + c \sin^2 \theta \cos^2 \theta$; and D: $a + b P_2^2(\cos \theta) + c \sin^2 \theta \cos^2 \theta$. These plots are fits for the β position of the 5 wt. % sample.

5.5 Errors

The relaxation times were all assumed to be single exponentials since the \ln of the Fourier transformed intensities of each peak was very close to a straight line. A Gauss-Newton method of least-squared fitting was used to determine the standard errors in the fits and these were used as the error in the relaxation times.

Chapter 6

Discussion

The quadrupolar splittings of the α , β and γ deuterons show different dependencies on water content (Figure 5.1). The $\Delta\nu_q$ of the α deuterons tends to increase with addition of PEG whereas $\Delta\nu_q$ for the β deuterons decreases. The γ deuterons show no real change in $\Delta\nu_q$. These results agree with previous findings [Bech 91] on POPC (1-palmitoyl-2-oleoyl-*sn*-glycero-3-phosphocholine) with the α and β positions deuterated. Since the direction of the shift in $\Delta\nu_q$ is different for the α and β deuterons, a simple increase or decrease in the disordering of the headgroup can not explain the results. This would cause a shift of $\Delta\nu_q$ in the same direction for all deuteron positions. Instead it is likely that a conformational change takes place in the average orientation of the headgroup. Bechinger and Seelig [Bech 91] suggest that the ^+N end of the phosphocholine dipole moves towards the interior of the bilayer upon dehydration.

The transition temperature increased as the amount of water in the bilayer decreased (Figure 5.2). As water is removed, motions such as rapid lateral diffusion and chain trans-gauche isomerizations which characterize the liquid crystalline phase are inhibited and more energy is required to get the same degree of motion as a fully hydrated lipid. Therefore, a higher temperature is needed to provide this energy in the liquid crystalline phase and thus the transition temperature increases. The results are consistent with many other experiments [Jurg 83, Koda 82]. Using the phase diagram of DPPC at low water content [Jurg 83], the actual number of water molecules in my study could be estimated by comparing my transition temperatures with the ones found in that paper.

Table 6.1: Conversion of wt. % PEG to no. of water molecules/lipid

wt. % PEG	no. H ₂ O molecules/lipid
10	full hydration (>10)
20	full hydration (>10)
30	7.4 - full (>10)
40	6.9 - 9.2
50	6.6 - 8.7
60	5.9 - 7.7
65	5.7 - 7.2
70	5.3 - 6.9
75	4.8 - 6.5
90	4.5 - 6.2

The results show that the number of water molecules per lipid ranged from greater than 10 (i.e. full hydration) for the 10 wt. % sample to between 4.5 and 6 for the 80 wt. % sample (Table 6.1). The fact that full hydration is still present at 30 wt. % PEG is due to the insensitivity of NMR in measuring small changes in T_m close to full hydration. The definition of full hydration is different here than elsewhere since the shift in transition temperature is insensitive to changes in the number of water molecules per lipid greater than 10 (i.e. 30 wt. % PEG). This means that as far as can be measured from changes in the transition temperature, the sample is fully hydrated at 30 wt. % PEG or less.

Another group [Cevc 85] did calculations on the change in T_m as the bilayer dehydrates and they found that the number of water molecules per lipid was directly proportional to the temperature shift. In these experiments, it was found that the shift in T_m was proportional to the square of the wt. % PEG (Figure 5.3). Also, Cevc and Marsh determined that the shift in T_m is smaller for lipids with longer chain length. Since my experiments with DMPC only involve samples at full hydration and at 50 wt. % PEG, investigation of the chain length dependence of T_m is incomplete. Comparison of only the 5 and 50 wt. %, samples for both the DMPC and DPPC do show a similar shift in

T_m equal to 4 K. This results seems reasonable since the difference in chain length is not great between the two lipids.

The longitudinal relaxation rates showed a decrease in T_{1z} by approximately 20% with the addition of a high wt. % PEG. This is surprising since another result in a similar system showed a linear increase in relaxation times upon addition of water [Ulri 90]. Their experiments on DOPC-d₉ (dioleoylphosphatidylcholine, deuterated in the choline methyl groups) showed a change in T_{1z} relaxation times from 20 ms at 5 water molecules per lipid to 65 ms for fully hydrated bilayers. One reason for this variation may be due to the difference in transition temperature between the two lipids. DOPC has a T_m of -20°C and the experiments by Ulrich *et al* were carried out at 30°C. DPPC has a transition temperature of 43°C and my experiments were done between 5°C and 7°C above T_m .

Neither T_{1z} nor T_{1q} show much anisotropy for the different headgroup deuterons. Similar results have been obtained in DPPC [Bloo 91b].

For the T_2 relaxation times, the orientation dependence was fit to a superposition of three mechanisms. In equation 5.4, the coefficient b represents fluctuation in the thickness of the bilayer or, equivalently, changes in the area of the lipids. The coefficient c represents undulations of the bilayers which causes a change in the director normal. The a coefficient represents motions which involve only single lipids, e.g. rotation about the long axis of the lipid and motion of the lipid into and out of the bilayer. The fit of Eq. 5.4 to the experimental data gave positive values for each of the coefficients, a necessary condition to be satisfied on physical grounds. From the results of the DMPC oriented samples, it seems impossible to isolate one specific motion which dominates the spectrum. Instead, all three motions seem to contribute to the angular dependence of longitudinal relaxation. Also, there does not appear to be any systematic suppression or enhancement of one type of motion with membrane dehydration since there is no consistent change in the a , b and c parameters between the 5 and 50 wt. % samples. It is

possible that both of the motions proposed here are coupled and therefore the presence of one automatically means the presence of another.

A problem with this analysis is that $P_2(\cos \theta)^2$ and $\sin^2 \theta \cos^2 \theta$ are not orthogonal. Therefore, the errors associated with the a , b and c coefficients are dependent on one another which was not taken into account in the fitting routine. An orthogonal set for this case is the even Legendre polynomials up to order four. These were fitted to the data (Table 5.4) but specific motions can not, at this time, be determined from the coefficients (which was the reason for the use of the other coefficients). The values for the a_0 , a_2 and a_4 coefficients can be used to determine the values of a , b and c . The comparison between the calculated and fitted values of a , b and c was very close which indicates that although the method of analysis may not be perfect, it is a good first step in understanding lipid motions.

Full hydration of the bilayer did seem to be achieved with a sample at 5 wt. % PEG since its values of T_m , $\Delta\nu$ and T_{1z} relaxation times were close to the ones for the powder sample. This is similar to other results using PEG to hydrate the bilayer [Morr 93b] where again a 5 wt. % PEG sample was assumed to be fully hydrated. Unfortunately, even with the comparison of T_{1z} relaxation times from the powder and oriented samples (which appears to be the most sensitive test for dehydration), full hydration can not be directly measured. The 10 wt. % PEG sample also seemed to be at full hydration when the same experimental parameters were examined. Therefore, even if the 10 wt. % PEG sample is not quite fully hydrated (since the most sensitive test can only measure changes in hydration after a certain number of water molecules are removed from the bilayer), the 5 wt. % sample which has even more water associated with the bilayer should be at full hydration. This new method of adding a polymer to the surrounding solution seems to allow oriented bilayers to reach full hydration unlike the usual method of using water saturated vapour.

Chapter 7

Conclusion

The use of a polymer as a dehydrating agent seems to be very effective in controlling the hydration of a membrane. My results for quadrupolar splitting and transition temperature show the same trends as other experiments which use different methods for dehydrating the bilayer. Also, it seems, likely that full hydration is reached when only a small wt. % PEG solution is added to the bilayer.

The main purpose of dehydrating the membrane was to look for changes in the motions of the lipids. This was done by measuring relaxation rates. The longitudinal relaxation rates did not seem to show much change when water was removed from the system. The spin-spin relaxation rates also did not show any systematic change with the addition of more PEG. The orientation dependence of the spin-spin relaxation times was used to determine the types of motions present in the bilayer. It was found that one particular motion did not dominate this angular dependence but instead a sum of three motions could be used to fit the data reasonably well. Two of these motions are thickness fluctuations and thermal undulations of the bilayer. The third was a residual non-isotropic component which was likely to arise from single lipid motion.

With the development of this new technique for membrane dehydration, further experiments on the effect of bilayer dehydration can be carried out relatively simply.

Bibliography

- [Arno 90] Arnold Klaus, Zschoernig Olaf, Barthel Dieter and Herold Wolfram. "Exclusion of poly(ethylene glycol) from liposome surfaces". (1990) *Biochim. biophys. Acta* **1022**:303-310.
- [Bech 91] Bechinger B. and Seelig J. "Conformational changes of the phosphatidylcholine headgroup due to membrane dehydration. A ^2H -NMR study". (1991) *Chem. Phys. Lipids* **58**:1-5.
- [Bloo 91a] Bloom, Myer and Evans, Evan. "Observation of surface undulations on the mesoscopic length scale by NMR". (1991) in *Biologically Inspired Physics* (ed. L. Peliti), pp. 137-147. New York: Plenum Press. 171.
- [Bloo 91b] Bloom, M., Morrison, C., Sternin, E. and Thewalt, J. "Spin echoes and the dynamic properties of membranes". (1991) In *Erwin Hahn - The Book*, (ed. D.M.S. Bagguley). London: Oxford University Press. 171.
- [Bush 80] Bush, S. Fowler, Adams, Ralph G. and Levin, Ira W. "Structural reorganization in lipid bilayer systems: effect of hydration and sterol addition on Raman spectra of dipalmitoylphosphatidylcholine multilayers". (1980) *Biochemistry* **19**:4429-4436.
- [Cevc 85] Cevc, Gregor and Marsh, Derek. "Hydration of noncharged lipid bilayer membranes". (1985) *Biophysical J.* **47**:21-31.
- [Davi 79] Davis, J.H. "Deuterium magnetic resonance study of the gel and liquid

- crystalline phases of dipalmitoylphosphatidylcholine". (1979) *Biophys. J.* **27**:339-358.
- [Davi 83] Davis, J.H. "The description of membrane lipid conformation, order and dynamics by ^2H NMR". (1983) *Biochim. biophys. Acta* **737**:117- 171.
- [Fine 74] Finer, E. G. and Darke A. "Phospholipid hydration studied by deuteron magnetic resonance spectroscopy". (1974) *Chem. Phys. Lipids* **12**:1-16.
- [Jeen 67] Jeener, J. and Broekaert, P. "Nuclear magnetic resonance in solids: thermodynamic effects of a pair of rf pulses". (1967) *Phys. Rev.* **157**:232-240.
- [Jurg 83] Jürgens E., Höhne G. and Sackmann E. "Calorimetric study of the dipalmitoylphosphatidylcholine / water phase diagram". (1983) *Ber. Bunsenges. Phys. Chem.* **87**:95-104.
- [Koda 82] Kodama, Michiko, Kuwabara Mika and Seki, Syûzô. "Successive phase transition phenomena and phase diagram of the phosphatidylcholine-water system as revealed by differential scanning calorimetry". (1982) *Biochim. biophys. Acta* **689**:567-570.
- [LeNe 77] LeNeveu D. M., Rand. R. P., Parsegian V. A. and Gingell D. "Measurement and modification of forces between lecithin bilayers". (1977) *Biophysical J.* **18**:209-229.
- [MacD 85] MacDonald Ruby I. "Membrane fusion due to dehydration by polyethylene glycol, dextran, or sucrose". (1985) *Biochemistry* **24**:4058-4066.
- [Morr 93a] Morrison, Clare and Bloom, Myer. "General orientation dependence of NMR spin-lattice relaxation for spin-1". (1993) *J. magn. Res.* In press.

- [Morr 93b] Morrison, Clare. "Polyethylene glycol as a hydration agent in oriented membrane bilayer samples". (1993) *Biophys. J.* In press.
- [Pfei 89] Pfeiffer, W., Henkel, Th., Sackmann, E., Knoll, W. and Richter, D. "Local dynamics of lipid bilayers studied by incoherent quasi-elastic neutron scattering". (1989) *Europhys. Lett.* **8**:201-206.
- [Rand 89] Rand, R. P. and Parsegian, V. A. "Hydration forces between phospholipid bilayers". (1989) *Biochim. biophys. Acta* **988**:351-376.
- [Ster 83] Sternin, E., Bloom, M. and MacKay, A. L. "De-pake-ing of NMR spectra". (1983) *J. magn. Res.* **55**:274-282.
- [Ster 85] Sternin, E. "Data acquisition and processing: a systems approach". (1985) *Rev. Sci. Instrum.* **56**:2043-2049.
- [Ulri 90] Ulrich A. S., Volke F. and Watts A. "The dependence of phospholipid head-group mobility on hydration as studied by deuterium-NMR spin-lattice relaxation time measurements". (1990) *Chem Phys. Lipids* **55**:61-66.